NASA Contractor Report 195044

ICASE Report No. 95-10

# ICASE

## UNIFICATION OF SOME ADVECTION SCHEMES IN TWO DIMENSIONS



D. Sidilkover
P. L. Roe



Contract No. NAS1-19480
February 1995



Institute for Computer Applications in Science and Engineering
NASA Langley Research Center
Hampton, VA 23681-0001

Operated by Universities Space Research Association

# UNIFICATION OF SOME ADVECTION SCHEMES IN TWO DIMENSIONS*

**D. Sidilkover**

*Institute for Computer Applications in Science and Engineering*
*NASA Langley Research Center*
*Hampton, VA 23681-0001*

and

**P. L. Roe**

*Department of Aerospace Engineering*
*University of Michigan*
*Ann Arbor, MI 48109*



## ABSTRACT

In this paper a relationship between two approaches towards construction of genuinely two-dimensional upwind advection schemes is established. One of these approaches is of the control volume type applicable on structured cartesian meshes. It resulted (see [14], [15]) in the compact high resolution schemes capable of maintaining second order accuracy in both homogeneous and inhomogeneous cases. Another one is the fluctuation splitting approach (see [11], [3], [12], [17]), which is well suited for triangular (and possibly) unstructured meshes. Understanding the relationship between these two approaches allows us to formulate here a new fluctuation splitting high resolution (i.e. possible use of artificial compression, while maintaining positivity property) scheme. This scheme is shown to be linearity preserving in inhomogeneous as well as homogeneous cases.

*The first author was supported by DOE grant DE-FG02-92ER25139, while he was in residence at Courant Institute of Mathematical Sciences, 251 Mercer St., New York University, New York, NY 10012. Both authors were also supported in part by the National Aeronautics and Space Administration under NASA Contract No. NAS1-19480 while in residence at the Institute for Computer Applications in Science and Engineering (ICASE), NASA Langley Research Center, Hampton, VA 23681-0001.

## 1. Introduction

The perfect scheme for numerical advection still awaits discovery. Its attributes should include high accuracy in regions of smooth flow, together with some positivity property that avoids over- and undershoots near discontinuities. It is well known that these two properties are not both attainable within the class of linear schemes. This implies that successful schemes must be non-linear, (i.e. data dependent).

Thus the scheme must be furnished with a monitor function that measures the local smoothness of the data, for example by comparing consecutive gradients, as in the flux-limiter approach. This enlarges the stencil of the scheme beyond the minimum needed to attain a given formal accuracy. Such enlargement is undesirable for parallel implementation, and seems to impair the convergence of multigrid methods, as well as requiring supplementary conditions close to boundaries.

In [15] a monitor function was introduced that compares gradients in different directions. This led to an advection scheme of the control-volume type with a minimally-enlarged stencil, and with good multigrid capabilities. Recently, there has also been developed the class of "fluctuation-splitting" schemes. These schemes are intended to be coded as a loop over triangular (tetrahedral) elements, employing no data external to the triangle. Several non-linear variants of this technique have been devised that preserve positivity.

In this paper we show a strong relationship between the two types of schemes. In fact, for linear advection on regular grids, certain schemes in each class turn out to be identical. This enables the transfer of insights and techniques from one class to the other.

§2 presents some basic definitions and principles regarding the discretization of a conservation law. §3 documents several schemes of the control volume type, and shows how limiter functions can be introduced into them. §4 briefly describes the fluctuation-splitting approach, with some of the previously-employed positivity devices. §5 reformulates the nonlinear fluctuation-splitting schemes as limiter schemes and demonstrates their identity with some control-volume schemes. The performance of the fluctuation-splitting schemes is illustrated by some numerical experiments in §6. The conclusions of this work are presented in §7.

The truly two-dimensional control-volume advection scheme that is capable of producing second order accurate steady-state solutions for the case of a non-zero source term is formulated following [15] in Appendix A. The high-resolution fluctuation-splitting counterpart of this scheme is constructed in Appendix B.

## 2. Conservation law and its discretization

Consider the scalar conservation law

$$u_t + \vec{\nabla} \cdot \vec{\mathcal{F}} = s, \tag{2.1}$$

where $\vec{\mathcal{F}} = (f, g)$, and its nonconservative form, in which $\vec{\lambda} = (f_u, g_u)$

$$u_t + \vec{\lambda} \cdot \vec{\nabla} u = s. \tag{2.2}$$

In what follows, unless otherwise stated, we take $\vec{\lambda} = (a, b)$, with $a, b$ constant

$$(\partial_t + a\partial_x + b\partial_y)u = s. \tag{2.3}$$

This assumption does not impair the generality of the construction. This is because using the conservative linearization procedure developed in [2] general nonlinear conservation laws can be represented locally by a linear constant coefficient advection equation of the form (2.3).

We are interested here in the steady-state solutions (2.1), i.e. the case when $\partial_t u = 0$.

It will appear very useful to note that a steady-state solution of Eq.(2.1) in the homogeneous case ($s \equiv 0$, the case considered through the entire paper, except for the Appendix) has the following property: it is constant along the direction of the convection velocity (characteristic direction).

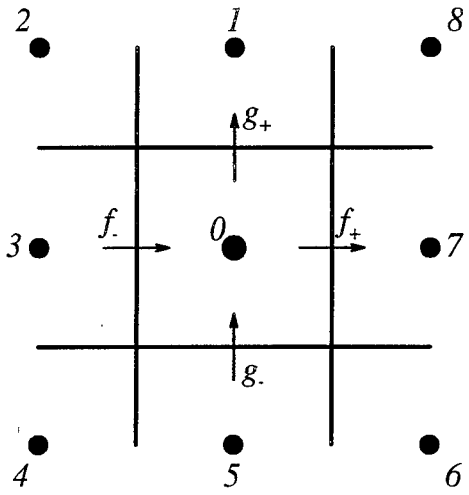

FIGURE 1. Control volume.

The time stepping (forward Euler) procedure is considered here to be only a means to reach the steady-state. The solution update formula can be given by the following

$$u_i^{n+1} = u_i^n - \frac{\Delta t}{h} \sum_k c_k (u_i^n - u_k^n), \tag{2.4}$$

i.e. the solution value in each grid point at the new time level can be represented as a combination of the solution values from the previous time level.

Applying the TVD concept to characterize the schemes producing non-oscillatory solutions appears to be too restrictive in two dimensions (see [4]). Therefore, we shall follow Spekreijse [16] and use the concept of positivity.

**Definition 2.1.** A scheme is said to be of the *positive* type if the solution update formula can be written in the form (2.4) in such a way that $c_k \geq 0, \quad \forall k$.

Solutions obtained by the means of positive schemes will satisfy a certain maximum principle.

## 3. CONTROL VOLUME APPROACH

Assume that the computational domain is divided into square cells (control volumes) each one associated with the cell-averaged value of the solution approximation (see Fig.1). Integrating Eq.(2.1) over a control volume and applying Gauss theorem we obtain

$$\iint_{C_0} u_t \, dxdy + \oint_{\partial C_0} u\vec{\lambda} \cdot d\vec{n} = \iint_{C_0} s \, dxdy \tag{3.1}$$

Since our purpose is to construct a second order accurate advection scheme, it is sufficient to approximate Eq.(3.1) using one- and two- dimensional mid-point quadrature rules. Thus, we obtain

$$u_0^{n+1} = u_0^n - \frac{\Delta t}{h}[f_+ - f_- + g_+ - g_-] + s_0 \Delta t, \tag{3.2}$$

where $f_+, f_-, g_+, g_-$ are numerical fluxes computed at the centers of each side of the control volume $C_0$. The question is how to compute them in order to obtain an advection scheme with desired properties.

In order to simplify our further discussion in this section we assume that

$$0 \leq a \leq b \tag{3.3}$$

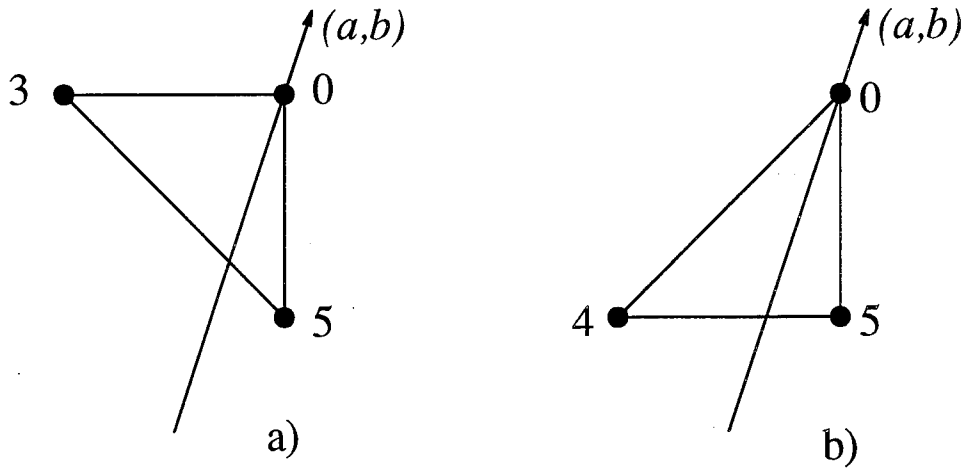


FIGURE 2. Stencils of the first order schemes: a) dimensional upwinding: b) N scheme.

3.1. **Dimensional upwinding.** The simplest example of a positive linear scheme is given by the dimensionally upwinded scheme $U$ with the following fluxes

$$\begin{aligned} f_-^U &= au_3 \\ g_-^U &= bu_5 \end{aligned} \tag{3.4}$$

This corresponds to the following update formula

$$u_0^{n+1} = u_0^n - \frac{\Delta t}{h}[b(u_0 - u_5) + a(u_0 - u_3)] \tag{3.5}$$

(Fig.2(a) presents the corresponding stencil). However, this scheme suffers from an excessive numerical diffusion.

3.2. **Zero cross-diffusion schemes.** Here we present the zero cross-diffusion 2D scheme that was used in [14],[15] for constructing a nonlinear zero cross diffusion positive scheme (see also §3.4 and §3.5). The fluxes are

$$\begin{aligned} f_-^{2D} &= au_3 - \tfrac{1}{2}b(u_3 - u_4) \\ g_-^{2D} &= bu_5 - \tfrac{1}{2}a(u_5 - u_4) \end{aligned} \tag{3.6}$$

These flux formulae can be motivated by considering the characteristics $dy/dx = b/a$ of (2.3). Specifically, produce the characteristic through the midpoint of the west face of the control volume, and find the value of $u$ on it by linear interpolation (or extrapolation) in the interval 34. Multiply this by $a$ to get $f_-$. Similarly the characteristic through the midpoint of the south face carries a value found from the data 45, that gives $g_-$ when multiplied by $b$. The additional terms found in these fluxes when compared with the $U$ scheme can be regarded as antidiffusive terms which compensate for the diffusivity of the upwind scheme. It is natural to think of creating a high-resolution scheme by applying limiters to these terms.

The update formula for this scheme is

$$\begin{aligned} u_0^{n+1} &= u_0^n - \frac{\Delta t}{h}[\frac{b}{2}(u_0 - u_5) - \frac{b}{2}(u_3 - u_4) + \frac{a}{2}(u_5 - u_4) - \frac{a}{2}(u_0 - u_3)] \\ &= u_0^n - \frac{\Delta t}{h}[\frac{b-a}{2}(u_3 - u_4 - u_0 + u_5) + b(u_0 - u_5) + a(u_5 - u_4)] \end{aligned} \tag{3.7}$$

(and its stencil is presented in Fig.3(a).

This scheme is not of the positive type – the coefficient multiplying $u_3$ in the update formula is negative in our representative case (3.3). Another defect of this scheme is that it will switch discontinuously when $a$ or $b$ changes sign.

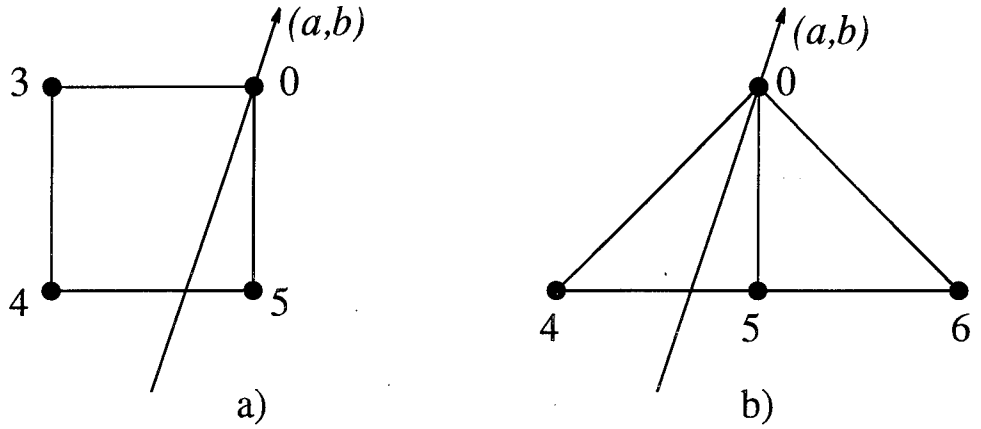

FIGURE 3. Stencils of the linear zero cross-diffusion schemes.

A steady-state solution for the homogeneous advection equation obtained by means of a zero cross diffusion scheme will be second order accurate [14],[5].

It must be noted that there is an arbitrariness in the flux formulae. A term $k(u_3 - u_4)$ can be added to $f_-$, and a term $k(u_4 - u_5)$ to $g_-$, without affecting the update formula, if $k$ is any constant. In fact, one of the flux values is arbitrary. In the remainder of this paper, we adopt, as in [13], a convention that if $b > a$ then $g$ is always given by the characteristic interpolation (3.6), but if $b < a$ it is $f$ that is found in this way.

3.3. **N scheme.** A positive, though first order accurate, modification of the scheme given by (3.6) is the following

$$\begin{aligned} f_-^N &= au_3 - \tfrac{1}{2}\min(a,b)(u_3 - u_4) \\ g_-^N &= bu_5 - \tfrac{1}{2}\min(a,b)(u_5 - u_4) \end{aligned} \tag{3.8}$$

or, because of our convention (3.3),

$$\begin{aligned} f_-^N &= au_3 - \tfrac{1}{2}a(u_3 - u_4) \\ g_-^N &= bu_5 - \tfrac{1}{2}a(u_5 - u_4) \end{aligned} \tag{3.9}$$

The corresponding update formula is (Fig.2(b) presents the corresponding stencil)

$$u_0^{n+1} = u_0^n - \frac{\Delta t}{h}[b(u_0 - u_5) + a(u_5 - u_4)] \tag{3.10}$$

This scheme was introduced by Rice and Schnipke [10] and was called the N (narrow) scheme in [14],[15] for its narrow stencil. Analysis in [13] shows that the N scheme is the optimal (in terms of cross diffusion) among the linear positive schemes in two dimensions.

It is interesting to note that Raithby's scheme [9] is in fact identical to the 2D scheme for the case $b/2 \le a \le b$. However, for $0 \le a \le b/2$ Raithby's scheme would correspond to a blend of the 2D scheme with the N scheme. The weight of the N scheme gradually increases with decreasing of $a/b$ and becomes equal to 1 when $a = 0$.

3.4. **S scheme.** In order to combine the positivity property with second order accuracy a non-linear scheme has to be constructed.

A positive zero cross diffusion scheme can be constructed in the way similar to TVD schemes in one dimensions. A "limited" zero cross diffusion correction is added to a first order accurate positive scheme. Such a scheme was developed in [14],[15] and was called the S scheme. It is a nonlinear modification of the scheme (3.6) and is given by the following fluxes

$$\begin{aligned} f_-^S &= f_-^N - \tfrac{1}{2}\Psi(R_{543})(b - a)(u_3 - u_4) \\ g_-^S &= g_-^N \end{aligned} \tag{3.11}$$

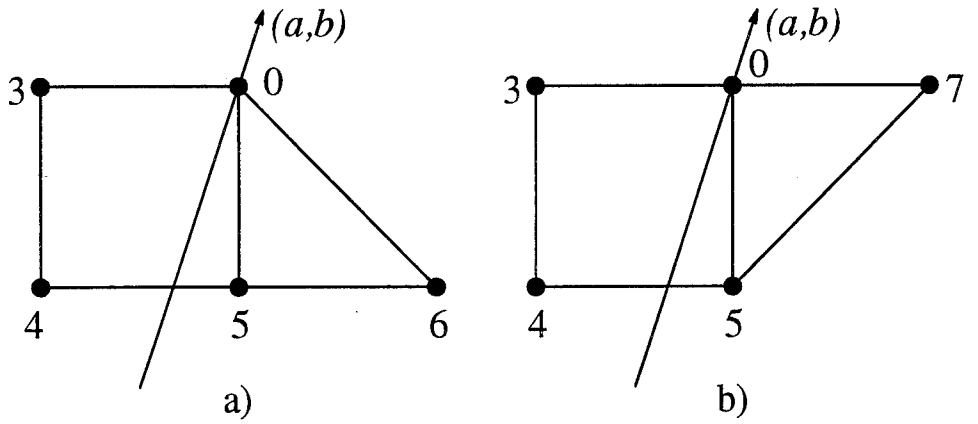


FIGURE 4. Positive (non-linear) zero cross-diffusion schemes: a) S scheme; b) S* scheme.

The ratio $R_{ijk}$ is defined by

$$R_{ijk} = -\frac{a(u_i - u_j)}{b(u_k - u_j)} \tag{3.12}$$

Here $i, j$ are some pair of grid points consecutive in the $x$-direction, and $j, k$ are consecutive in the $y$-direction. Thus, in smooth regions where the solution is close to convergence, $R_{ijk} \simeq 1$. This quantity is an example of a two-dimensional smoothness monitor. In particular

$$R_{543} = -\frac{a(u_5 - u_4)}{b(u_3 - u_4)} \tag{3.13}$$

and $\Psi(R)$ is a limiter [1] function [18] having the property $\Psi(1/R) = \Psi(R)/R$. Note that the limiting is applied to the difference between the fluxes of the 2D and N schemes.

$$u_0^{n+1} = u_0^n - \frac{\Delta t}{h}\begin{bmatrix} b(u_0 - u_5) + a(u_5 - u_4) \\ +\frac{1}{2}\Psi(R_{543})(b-a)(u_3 - u_4) \\ -\frac{1}{2}\Psi(R_{650})(b-a)(u_0 - u_5) \end{bmatrix} \tag{3.14}$$

Using the following identity

$$\Psi(R_{543})b(u_3 - u_4) \equiv -\frac{\Psi(R_{543})}{R_{543}}a(u_5 - u_4) \tag{3.15}$$

we can rewrite (3.14) as follows

$$u_0^{n+1} = u_0^n - \frac{\Delta t}{h}\begin{bmatrix} (b-a)\left(1 - \frac{1}{2}\Psi(R_{650}) + \frac{1}{2}\frac{\Psi(R_{543})}{R_{543}}\right)(u_0 - u_5) \\ +a\left(1 - \frac{1}{2}\frac{\Psi(R_{543})}{R_{543}}\frac{(b-a)}{b}\right)(u_0 - u_4) \end{bmatrix} \tag{3.16}$$

It is clear from (3.16) that the S scheme is of the positive type if

$$0 \le \frac{\Psi(R)}{R} \le 2, \quad 0 \le \Psi(R) \le 2. \tag{3.17}$$

It was also shown in [14],[15] that the S scheme is second order accurate for a steady-state solution

[1] For any $\Psi$ of this form, we can write $\Psi(P/Q) = M(P,Q)/Q = M(Q,P)/Q = P/Q \cdot \Psi(Q/P)$, where $M$ is some averaging function having the symmetry property $M(P,Q) = M(Q,P)$. The forms involving $M$ are preferable for coding, because they do not break down when $P \simeq Q \simeq 0$.

of a homogeneous advection equation (i.e. it has a zero cross diffusion) if $\Psi$ is Lipschitz continuous and

$$\Psi(1) = 1. \tag{3.18}$$

*Remark 3.1.* The S scheme relies on a 5-point stencil (see Fig.4(a)) - just one point more than the linear zero cross-diffusion scheme (3.6). This one extra point was needed to achieve positivity.

It is remarkable that the choice of limiter function in order to obtain a positive scheme with zero cross-diffusion is dictated by relations (3.17) and (3.18) which are identical to those arising when constructing one-dimensional TVD-type schemes. Therefore, most of the limiters used in one dimension (see [18]) can be used in the present context as well.

*Remark 3.2.* Another zero cross diffusion scheme was presented by Koren [7]

$$\begin{aligned} f_{-}^{T} &= f_{-}^{N} + \tfrac{1}{2}\tfrac{a(b-a)}{b}(u_5 - u_4) \\ g_{-}^{T} &= g_{-}^{N} \end{aligned} \tag{3.19}$$

The update formula is

$$u_0^{n+1} = u_0^n - \frac{\Delta t}{h}\begin{bmatrix} \tfrac{1}{2}\tfrac{a(b+a)}{b}(u_5 - u_4) \\ +b(u_0 - u_5) \\ +\tfrac{1}{2}\tfrac{a(b-a)}{b}(u_6 - u_5) \end{bmatrix} \tag{3.20}$$

The advantage of this scheme is that it switches continuously when $a$ changes sign.

It can be easily seen that this scheme is identical to the one-dimensional Lax-Wendroff scheme, assuming that $y$ is the time-like direction.

A detailed analysis of the class of zero cross diffusion schemes was done by Hirsch [5]. It is also proved there that a linear scheme with zero cross diffusion cannot be of the positive type, thus generalizing Godunov's theorem to two dimensions.

*Remark 3.3.* An alternative route to a positive zero cross diffusion scheme is through the nonlinear modification of the scheme (3.19)

$$\begin{aligned} f_{-}^{T} &= f_{-}^{N} + \tfrac{1}{2}\tfrac{\Psi(R_{543})}{R_{543}}\tfrac{a(b-a)}{b}(u_5 - u_4) \\ g_{-}^{T} &= g_{-}^{N}. \end{aligned} \tag{3.21}$$

However, it is easy to see using (3.15) and assuming a symmetry property for the limiter, i.e.

$$\frac{\Psi(R)}{R} \equiv \Psi(\frac{1}{R}) \tag{3.22}$$

(and most of the commonly used limiters are symmetric, see [18]), that the scheme (3.21) is *identical* to the S scheme.

*Remark 3.4.* The choice of the ratio that the limiter function can rely on is non-unique. For instance, the upwind positive scheme with zero cross-diffusion presented by Hirsch & Van Ransbeeck [6] has a limiter function with the following ratio as its argument

$$R_{034} = -\frac{a(u_0 - u_3)}{b(u_3 - u_4)} \tag{3.23}$$

3.5. **S* scheme.** One of the main objectives of this work is to establish links between the control volume and fluctuation-splitting approaches towards the construction of the truly two-dimensional advection schemes. It is important for this purpose to introduce the scheme S* which has a more 'triangular flavor'. The limiter schemes above are based on ratios $R_{ijk}$ of gradients in orthogonal directions. Now we introduce the ratio $R^*_{ijk}$, defined as

$$R^*_{ijk} = \frac{-a(u_i - u_j)}{(b-a)(u_k - u_j)} \tag{3.24}$$

where the pair of points $j, k$ are adjacent along a diagonal. The fraction has been normalized so that we still have $R^*_{ijk} \simeq 1$ for smooth, nearly steady solutions.

The $S^*$ scheme can be defined by the following numerical fluxes

$$\begin{array}{rcl} f^{S^*}_{-} & = & f^N_{-} - \frac{1}{2}\Psi(R^*_{043})(b-a)(u_3 - u_4) \\ g^{S^*}_{-} & = & g^N_{-} \end{array} \tag{3.25}$$

with

$$R^*_{043} = -\frac{a(u_0 - u_4)}{(b-a)(u_3 - u_4)}). \tag{3.26}$$

The update formula in this case is (the stencil is presented in Fig.4(b))

$$u_0^{n+1} = u_0^n - \frac{\Delta t}{h}\left[\begin{array}{r} b(u_0 - u_5) + a(u_5 - u_4) \\ +\frac{1}{2}\Psi(R_{043})(b-a)(u_3 - u_4) \\ -\frac{1}{2}\Psi(R_{750})(b-a)(u_0 - u_5)] \end{array}\right] \tag{3.27}$$

Note that the following identity holds

$$\Psi(R_{043})(b-a)(u_3 - u_4) \equiv -\frac{\Psi(R_{043})}{R_{043}} a(u_0 - u_4). \tag{3.28}$$

**Lemma 3.5.** *If the limiter $\Psi = \Psi(R)$ satisfies the following inequality*

$$0 \le \frac{\Psi(R)}{R} \le 2, 0 \le \Psi(R) \le 2. \tag{3.29}$$

*then the S* scheme is of positive type.*

*Proof.* Using the identity (3.28) the update formula for the S* scheme can be rewritten as follows

$$u_0^{n+1} = u_0^n - \frac{\Delta t}{h}\left[\begin{array}{r} (b-a)\left(1 - \frac{1}{2}\Psi(R_{750})\right)(u_0 - u_5) \\ +a\left(1 - \frac{1}{2}\frac{\Psi(R_{043})}{R_{043}}\right)(u_0 - u_4) \end{array}\right] \tag{3.30}$$

It is obvious from (3.30) that the scheme is positive if the inequality (3.29) holds. □

**Lemma 3.6.** *If $\Psi(R)$ is Lipschitz continuous and*

$$\Psi(1) = 1, \tag{3.31}$$

*then the S* scheme has a zero cross diffusion.*

*Proof.* This lemma is a simple corollary of Lemma A.1 concerning the more general scheme constructed for the inhomogeneous equation. □

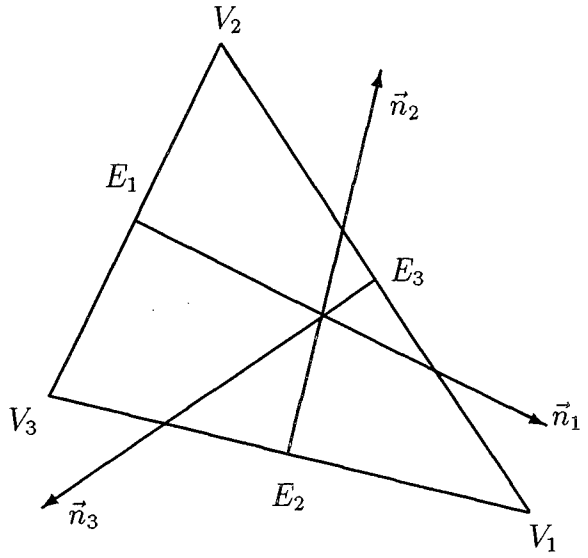


FIGURE 5. Illustration for construction of fluctuation-splitting schemes.

## 4. FLUCTUATION SPLITTING APPROACH

In this section we present a brief description of a fluctuation splitting approach. For more details see [3],[12],[17]. The schemes are designed for use on unstructured grids and their description is initially given in that context. Later, to compare with the control-volume approach, we specialize to structured grids, and later still we reconsider the general case.

Consider a numerical solution of the two dimensional linear constant coefficient advection equation

$$u_t + \vec{\lambda} \cdot \vec{\nabla} u = s. \tag{4.1}$$

The grid is taken to be an arbitrary triangulation of the domain. A typical element $T$ of such a grid is shown on Fig.5. The integral of $u_t$ over the triangle $T$ is called the "fluctuation"

$$\phi^T = \iint_T u_t dx dy. \tag{4.2}$$

Taking into account Eq.(4.1) and applying Gauss' theorem we obtain

$$\phi^T = \oint_{\partial T} u \vec{\lambda} \cdot d\vec{n} - \iint_T s \, dx dy, \tag{4.3}$$

where $\partial T$ is the boundary of the triangle $T$ and $d\vec{n}$ is the *inward* scaled normal to an element of the boundary. Assuming that the source term $s$ varies linearly within triangle $T$ we get

$$\sigma_T = \iint_T s \, dx dy = \frac{1}{3} S_T \sum_{i=1}^{3} s_i, \tag{4.4}$$

where $S_T$ is the area of the triangle $T$. We shall return to the inhomogeneous case in Appendix B. Here we assume that $s \equiv 0$ (and therefore $\sigma_T = 0$).

$$u_t + \vec{\lambda} \cdot \vec{\nabla} u = 0. \tag{4.5}$$

Assuming also that $u$ varies linearly within triangle $T$ we get

$$\phi^T = \frac{1}{2}(u_1 + u_2)\vec{\lambda} \cdot \vec{n}_3 + \frac{1}{2}(u_2 + u_3)\vec{\lambda} \cdot \vec{n}_1 + \frac{1}{2}(u_1 + u_3)\vec{\lambda} \cdot \vec{n}_2, \tag{4.6}$$

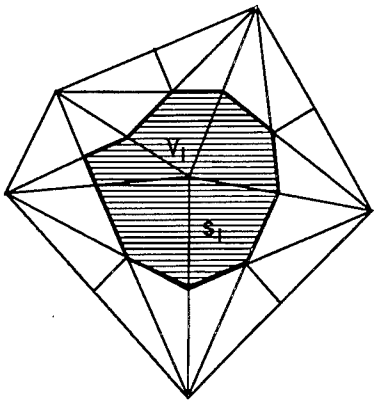


FIGURE 6. Median dual cell.

where

$$k_i = \frac{1}{2}\vec{\lambda} \cdot \vec{n}_i \tag{4.7}$$

and $\vec{n}_i$ is the inward normal to the side $E_i$ scaled with its length. Note that

$$\sum_{i=1}^{3} \vec{n}_i = 0 \tag{4.8}$$

and therefore

$$\sum_{i=1}^{3} k_i = 0. \tag{4.9}$$

This allows (4.6) to be rearranged as

$$\phi^T = -\sum_{i=1}^{3} k_i u_i. \tag{4.10}$$

Several alternative expressions can be obtained for $\phi^T$ using (4.9), for example,

$$\begin{aligned} \phi^T &= -k_2(u_2 - u_1) - k_3(u_3 - u_1) \\ &= -k_3(u_3 - u_2) - k_1(u_1 - u_2) \\ &= -k_1(u_1 - u_3) - k_2(u_2 - u_3) \end{aligned} \tag{4.11}$$

The computed fluctuation should then be distributed (split) among the vertices of the triangle $T$

$$S_i u_i := S_i u_i + \alpha_i^T \Delta t \phi^T, \qquad i = 1, 2, 3, \tag{4.12}$$

where $S_i$ is one-third the area of all the triangles having $V_i$ as a vertex (the area of so-called median dual cell of area $S_i$ around $i$, see Fig.6) and

$$\sum_{i=1}^{3} \alpha_i^T = 1. \tag{4.13}$$

The latter is necessary for the discretization to be conservative (see [3]).

After adding contributions from all the triangles $T$ having a common vertex at point $i$, we obtain the following scheme

$$u_i^{n+1} = u_i^n + \frac{\Delta t}{S_i} \sum_T \alpha_i^T \phi_T \tag{4.14}$$

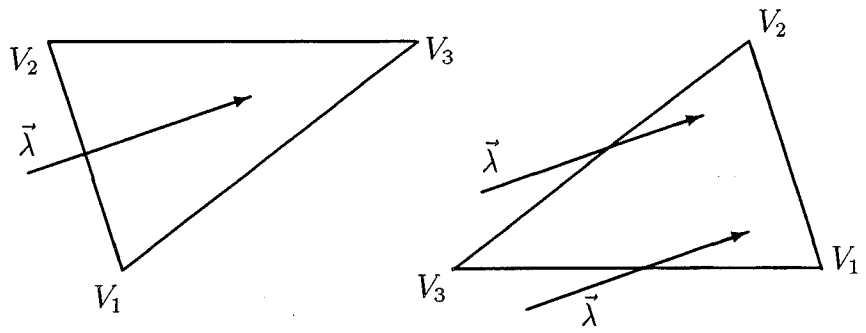


(a) Type I triangle (b) Type II triangle

FIGURE 7. Two possible triangle orientation with respect to the flow direction.

We assume here that each triangle sends contributions to its own vertices only. Therefore, the resulting scheme for $u_i$ has a compact stencil restricted to at most the immediate neighbours of $u_i$. The remaining question is how to chose $\alpha_i^T$.

An additional consideration is *positivity* of the constructed scheme. We will define a more restrictive condition of *local positivity* that requires contributions of each triangle separately to be positive.

**Definition 4.1.** In equation(4.12) choose from the preceding list the $i^{\text{th}}$ definition of $\phi^T$, so that

$$S_i u_i := S_i u_i - \alpha_i[k_j(u_j - u_i) + k_k(u_k - u_i)]. \tag{4.15}$$

Then the scheme is said to be locally positive if the three quantities

$$-\alpha_i k_j \Delta t, \quad -\alpha_i k_k \Delta t, \quad 1 + \alpha_i(k_j + k_k)\Delta t$$

are all positive

This condition is easier to implement because it retains the basic property of a fluctuation-splitting scheme that all triangles can be processed without reference to any other data. However, it is more restrictive than necessary because it does not recognise that compensating changes from other triangles may restore positivity. It is the condition currently used in design of fluctuation splitting schemes. Application of the *non-local* positivity condition may allow addition of artificial compression to the scheme. This will be discussed in §5.2.

**Definition 4.2.** The fluctuation-splitting scheme is called linearity preserving if whenever the fluctuation on the triangle T vanishes then the scheme leads to a zero update in each of the three vertices of the triangle.

It was observed by Deconinck et al [3] that linearity-preserving schemes give solutions that are second-order accurate in the steady state.

4.1. **N scheme.** This linear, positive, fluctuation splitting scheme is called the N scheme because it was found by Roe [12] that it is closely related to the control volume N scheme. (We shall return to this point in §5.1.1). Note that there exist two possibilities regarding $k_i$ for $i = 1, 2, 3$ (because of Eq.(4.9)): either one of them is positive and the rest are negative or two of them are positive and one negative. These two situations correspond to a triangle with either one inflow face or two inflow faces. Without loss of generality we can consider the following two cases (see Fig.7)

(a) : $k_1 < 0,\ k_2 < 0,\ k_3 > 0,$
(b) : $k_1 > 0,\ k_2 > 0,\ k_3 < 0.$

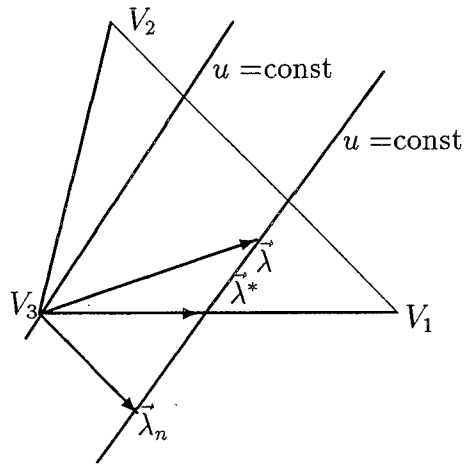


FIGURE 8. Construction of the NN scheme.

The obvious choice for the first case (Type I triangle) is to send the entire fluctuation to the downstream vertex 3 (i.e. setting $\alpha_1^T = \alpha_2^T = 0,\ \alpha_3^T = 1$ )

$$S_3 u_3^{n+1} = S_3 u_3^n - \Delta t[k_1(u_1 - u_3) + k_2(u_2 - u_3)] \tag{4.16}$$

Although interesting schemes can be created that do not follow this rule, we will assume for the remainder of this paper that all Type I triangles are dealt with like this.

Case (b) is more complicated. If the fluctuation is distributed according to the following formulae

$$\begin{aligned} S_1 u_1^{n+1} &= S_1 u_1^n - \Delta t[k_1(u_1 - u_3)] \\ S_2 u_2^{n+1} &= S_2 u_2^n - \Delta t[k_2(u_2 - u_3)] \end{aligned} \tag{4.17}$$

the resulting scheme is obviously positive and this will define the N sceme. Strong convergence of the N scheme on general triangulations is proved by Perthame [8]. However, it does not have the LP property. This is because the contributions to the residuals at both vertices 1 and 2 may be different from zero even if the fluctuation on triangle $T$ vanishes.

4.2. **NN scheme.** It was pointed out in [11],[3],[12] that replacing the advection velocity $\vec{\lambda}$ by its normal to the level lines component $\vec{\lambda}_n$ normal to the level lines (or tangential to the gradient direction) of $u$ within triangle T

$$\vec{\lambda}_n = (\vec{\lambda} \cdot \vec{\nabla} u) \cdot \frac{\vec{\nabla} u}{|\vec{\nabla} u|^2} \tag{4.18}$$

does not affect the residual. It is also obvious that substituting the advection velocity by the following

$$\vec{\lambda}^* = \vec{\lambda}_n + \theta \vec{\lambda} \tag{4.19}$$

does not affect the residual either. Defining

$$k_i^* = \frac{1}{2} \vec{\lambda}^* \cdot \vec{n}_i \tag{4.20}$$

and

$$\begin{aligned} S_1 u_1^{n+1} &= S_1 u_1^n - \Delta t[k_1^*(u_1 - u_3)] \\ S_2 u_2^{n+1} &= S_2 u_2^n - \Delta t[k_2^*(u_2 - u_3)] \end{aligned} \tag{4.21}$$

one can observe that if $\theta = 0$, the NN scheme (4.21) will be linearity preserving. This is because $\vec{\lambda}_n$ vanishes at the steady state (and therefore $k_1^*$ and $k_2^*$ vanish in this case). However, vector $\vec{\lambda}_n$ may extend out of triangle $T$ (Fig.8). Therefore, the scheme in this case is not positive, i.e. one of

the $k$'s in (4.21) will be negative. To obtain positivity of the scheme in this case $\theta$ should be taken such that the vector $\vec{\lambda}^*$ will be directed along the face of triangle $T$. This means that the entire residual should be sent to only one of the outflow nodes.

Because the effective advection speed is data dependent (when $\theta = 0$ it is the drift velocity of the contours) the NN scheme is nonlinear in a way that permits it to escape Godunov's Theorem. Although the mechanism involved appears very different from that employed by limiter schemes, we will see in the next section that a unification is possible.

It was pointed out in [3] that when the solution is almost a constant, the expression for $\vec{\lambda}_n$ (4.18) becomes ill-defined, which may affect the convergence. A way to overcome this difficulty suggested in [3] was to switch gradually from $\vec{\lambda}^*$ to $\vec{\lambda}$ in regions where the gradients are small.

4.3. **Level scheme.** It was argued by Roe in [12] that the NN scheme is not optimal in terms of the maximal allowed time step and another scheme for Type II triangles was suggested there. This scheme was later named the Level scheme.

A brief description of the algorithm is given here. The reader is referred to [12] for the complete derivation.

The residual is distributed among the nodes according to the following formulae:

$$\begin{aligned} S_1 u_1^{n+1} &= S_1 u_1^n + \Delta t \alpha_1 \phi_T \\ S_2 u_2^{n+1} &= S_2 u_2^n + \Delta t \alpha_2 \phi_T \end{aligned} \tag{4.22}$$

It is very interesting for the discussion in §5.1.3 to note that in [12] the following quantity

$$\Lambda = -\frac{u_1 - u_3}{u_2 - u_3} \tag{4.23}$$

was suggested to distinguish between two cases

(a) : $\Lambda \geq 0$, i.e. the level line passes through triangle $T$,
(b) : $\Lambda < 0$, i.e. the level line lies outside of triangle $T$.

In case (a) only one vertex is updated: the vertex that the characteristic line passes closer to it than the level line.

In case (b) both vertices are updated. The residual is distributed according to the following formulae

$$\begin{aligned} \alpha_1 &= \frac{S_1(u_1-u_3)}{S_1(u_1-u_3)+S_2(u_2-u_3)} \\ \alpha_2 &= \frac{S_2(u_2-u_3)}{S_1(u_1-u_3)+S_2(u_2-u_3)} \end{aligned} \tag{4.24}$$

This choice of $\alpha$'s is argued in [12] to be optimal in terms of the maximal allowed time step. Also, this choice preserves the direction of the level lines; hence the name of the scheme.

However, Deconinck [1] has observed that the Level scheme may switch discontinuously if $\vec{\lambda}$ is almost parallel to one side of the triangle, say side 1, but $(u_2-u_3)/(u_1-u_3) > 0$. This demonstrates that $\Lambda$ was an unhappy choice of parameter.

## 5. Unified approach

It is shown in this section that there is more in common between the two previously reviewed approaches than just a philosophy to make constructive use of nonlinearity. In fact the fluctuation splitting methodology and control volume compact scheme methodologies can be seen as two dual ways to interpret the same approach.

Consider the following scheme on Type II triangles

$$\begin{aligned} S_1 u_1^{n+1} &= S_1 u_1^n + \Delta t[k_1(u_1 - u_3) + \Psi(R_{132}) k_2(u_2 - u_3)] \\ S_2 u_2^{n+1} &= S_2 u_2^n + \Delta t[k_2(u_2 - u_3) - \Psi(R_{132}) k_2(u_2 - u_3)] \end{aligned} \tag{5.1}$$

where $R_{ijk}$ now compares contributions to the fluctuation from two sides of the triangle, i.e.

$$R_{ijk} = -\frac{k_i(u_i - u_j)}{k_k(u_k - u_j)}. \tag{5.2}$$

Again, we have $R_{ijk} \simeq 1$ for smooth, nearly steady flow.

$$R_{132} = -\frac{k_1(u_1 - u_3)}{k_2(u_2 - u_3)} \tag{5.3}$$

The conservation property of this scheme is obvious from (5.1).

We have the identity

$$\Psi(R_{132})k_2(u_2 - u_3) \equiv -\frac{\Psi(R_{132})}{R_{132}}k_1(u_1 - u_3) \tag{5.4}$$

**Theorem 5.1.** *If the limiter $\Psi(R)$ satisfies the following inequality*

$$0 \leq \frac{\Psi(R)}{R} \leq 1, \quad 0 \leq \Psi(R) \leq 1, \tag{5.5}$$

*then the NNL scheme is (locally) positive.*

*Proof.* Using the identity (5.4) the scheme (5.1) can be rewritten in the following form

$$\begin{array}{ll} S_1 u_1^{n+1} & = S_1 u_1^n + \Delta t[1 - \frac{\Psi(R_{132})}{R_{132}}]k_1(u_1 - u_3) \\ S_2 u_2^{n+1} & = S_2 u_2^n + \Delta t[1 - \Psi(R_{132})]k_2(u_2 - u_3) \end{array} \tag{5.6}$$

It can be concluded from the latter that the NNL scheme is positive if inequality (5.5) holds. □

*Remark 5.2.* By contrast to the control volume schemes, it is here possible only to use limiters for which the upper bound on $\Psi, \Psi/R$, is equal to 1.0 rather than 2.0. That is, the limiter cannot be compressive. We show later that compressive limiters can be allowed within the fluctuation splitting scheme given sufficient information about mesh connectivity.

**Theorem 5.3.** *The NNL scheme is linearity preserving if*

$$|\Psi(R) - 1| < C|R - 1|. \tag{5.7}$$

*for some positive constant $C$.*

*Proof.* We have

$$\begin{array}{llll} S_1 u_1^{n+1} - S_1 u_1^n & = \delta u_1 & = \Delta t[k_1(u_1 - u_3) + \Psi(R_{132})k_2(u_2 - u_3)] & = P + \Psi(R)Q \\ S_2 u_2^{n+1} - S_2 u_2^n & = \delta u_2 & = \Delta t[k_2(u_2 - u_3) + \frac{\Psi(R_{132})}{R_{132}}k_1(u_1 - u_3)] & = Q - \Psi(R)Q \end{array} \tag{5.8}$$

We wish to show that if $P + Q = 0$ then $\delta u_1 = \delta u_2 = 0$, or equivalently

$$|\delta u_1 - \delta u_2| < K|\delta u_1 + \delta u_2|,$$

for some positive constant $K$. Now, if

$$|\Psi - 1| < C|R - 1|$$

then

$$\begin{array}{rcl} 2|\Psi - 1||Q| & < & 2C|P + Q|, \\ |P + Q| + 2|\Psi - 1||Q| & < & (2C + 1)|P + Q|, \\ |P + Q + 2(\Psi - 1)Q| & < & (2C + 1)|P + Q|, \\ |P - Q + 2\Psi Q| & < & (2C + 1)|P + Q|. \end{array} \tag{5.9}$$

This last statement translates, with $K = 2C + 1$, into the one we want to prove. □

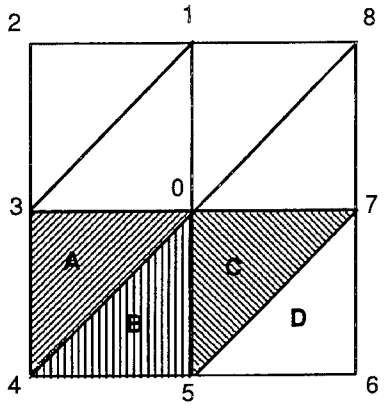


FIGURE 9. Possible triangulation of the Cartesian grid.

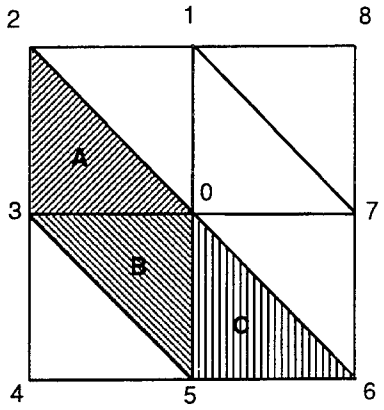


FIGURE 10. Possible triangulation of the Cartesian grid.

*Remark 5.4.* It is interesting to note that the NNL scheme with the "minmod" limiter is identical to the Level scheme in the case when the level line lies inside the triangle. To illustrate this assume that $R_{132} > 1$. For the minmod limiter this means that $\Psi(R_{132}) = 1$. It follows from (5.1) that the entire fluctuation contributes to the solution update at the node 1 - exactly what the Level scheme corresponds to.

## 5.1. **Links to the control volume approach.**

5.1.1. *N schemes.* Consider the grid as illustrated in Fig.9. The fluctuations for the triangles $A, B, C$ are given by the following expressions

$$\begin{aligned}
\phi^A &= -\tfrac{h}{2}[(b-a)(u_3-u_4) + \underline{a(u_0-u_4)}] \\
\phi^B &= -\tfrac{h}{2}[\underline{a(u_0-u_4)} + \underline{(b-a)(u_0-u_5)}] \\
\phi^C &= -\tfrac{h}{2}[a(u_7-u_5) + \underline{(b-a)(u_0-u_5)}]
\end{aligned}$$

The underlined terms here contribute to the residual at the node 0 according to (4.16),(4.17). Assembling all the contributions the following update is obtained

$$u_0^{n+1} = u_0^n + \frac{\Delta t}{h}[b(u_5-u_0) + a(u_4-u_0)] \tag{5.10}$$

It was pointed out by Roe [12] that (5.10) is identical in this case to the update formula for the control volume type N scheme (3.10). That is why these two schemes are called N schemes. Another interesting observation made in [12] is that if the N scheme is constructed on the triangulation

illustrated on Fig.10

$$\begin{aligned}\phi^A &= -\tfrac{h}{2}[(b-a)(u_3-u_4) + \underline{a(u_0-u_4)}]\\ \phi^B &= -\tfrac{h}{2}[\underline{a(u_0-u_4)} + \underline{(b-a)(u_0-u_5)}]\\ \phi^C &= -\tfrac{h}{2}[a(u_7-u_5) + \underline{(b-a)(u_0-u_5)}]\end{aligned}$$

it can be seen from the update formula

$$u_0^{n+1} = u_0^n + \frac{\Delta t}{h}[b(u_5-u_0) + a(u_3-u_0)] \tag{5.11}$$

that the scheme in this case is identical to the dimensional upwinding (3.5).

5.1.2. *2D scheme.* Consider again triangulation illustrated on Fig.9. The fluctuations on the triangles $A, B, C$ are again given as follows

$$\begin{aligned}\phi^A &= -\tfrac{h}{2}[\underline{(b-a)(u_3-u_4)} + \underline{a(u_0-u_4)}]\\ \phi^B &= -\tfrac{h}{2}[\underline{a(u_0-u_4)} + \underline{(b-a)(u_0-u_5)}]\\ \phi^C &= -\tfrac{h}{2}[a(u_7-u_5) + (b-a)(u_0-u_5)]\end{aligned}$$

Note, that now only triangles $A, B$ participate in the molecule at node 0, however they contribute their entire fluctuations. This would correspond, in the fluctuation-splitting approach, to a rule that each triangle only updates it's most downwind node (the one for which $\vec{\lambda}\cdot\vec{x}$ is maximum).

The update formula in this case

$$u_0^{n+1} = u_0^n + \frac{\Delta t}{h}[\frac{(a-b)}{2}(u_3-u_0) + \frac{(b-a)}{2}(u_5-u_0) + \frac{(a+b)}{2}(u_4-u_0)] \tag{5.12}$$

is identical to the 2D control volume scheme (3.7).

5.1.3. *Linearity preserving positive schemes.* Consider triangles $A, B, C$ as illustrated in Fig.9. Define

$$R_{043} = -\frac{a(u_0-u_4)}{(b-a)(u_3-u_4)}, \qquad R_{750} = -\frac{a(u_7-u_5)}{(b-a)(u_0-u_5)}. \tag{5.13}$$

The fluctuations on these triangles are

$$\begin{aligned}\phi^A &= -\tfrac{h}{2}\{[1-\Psi(R_{043})](b-a)(u_3-u_4) + \underline{a(u_0-u_4)} + \underline{\Psi(R_{043})(b-a)(u_3-u_4)}\}\\ \phi^B &= -\tfrac{h}{2}\{\underline{a(u_0-u_4)} + \underline{(b-a)(u_0-u_5)}\}\\ \phi^C &= -\tfrac{h}{2}\{a(u_7-u_5) + \Psi(R_{750})(b-a)(u_0-u_5) + \underline{[1-\Psi(R_{750})](b-a)(u_0-u_5)}\}\end{aligned} \tag{5.14}$$

The underlined terms contribute to the residual at the point 0

$$u_0^{n+1} = u_0^n + \frac{\Delta t}{h}\left[\begin{array}{r}\left((b-a) - \frac{1}{2}\Psi(R_{750})(b-a)\right)(u_5-u_0)\\ + \left(a + \frac{1}{2}\Psi(R_{043})(b-a)\right)(u_4-u_0)\\ + \left(-\frac{1}{2}\Psi(R_{043})(b-a)\right)(u_3-u_0)\end{array}\right] \tag{5.15}$$

which is identical to the update formula for the S* scheme (3.27)!

5.2. **Artificial compression.** Note that it was possible to use a compressive limiter [2] for the S* scheme. This was possible to show by requiring *non-local* positivity, which is a less restrictive requirement. If we were to restrict our attention only to structured grids, we could use the equivalence of the $S^*$ and $NNL$ schemes to justify using compressive limiters in the $NNL$ scheme also. We now discuss how compressive limiters may be employed when we know something about the connectivity of the grid.

Consider triangle $C$ (Fig.9). Collect from triangles $B$ and $C$ those terms in the fluctuations that contribute to the update at node 0 and contain a factor $(u_5-u_0)$.

[2] A compressive limiter can be defined as one for which the upper limit on $\Psi, \Psi/R$ is greater than unity.

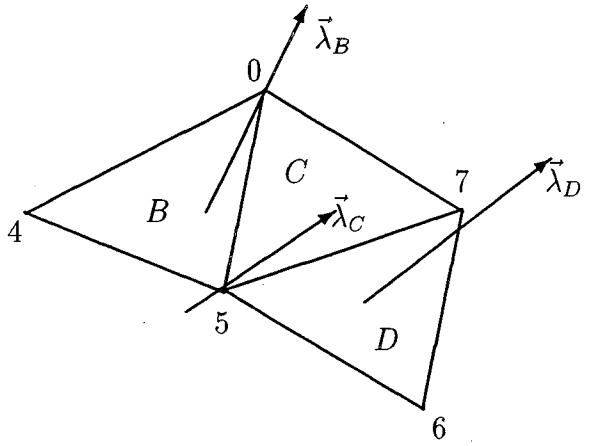


FIGURE 11. General triangulation.

$$\begin{aligned} \phi_0^B + \phi_0^C &= \frac{h}{2}\{[1 - \Psi(R_{750})](b-a)(u_5 - u_0) + (b-a)(u_5 - u_0)\} \\ &= \frac{h}{2}[2 - \Psi(R_{750})](b-a)(u_5 - u_0) \end{aligned} \tag{5.16}$$

Similarly, collect from triangles $D$ and $C$ those terms in the fluctuations that contribute to the update at node 7 and contain a factor $(u_5 - u_7)$.

$$\begin{aligned} \phi_7^C + \phi_7^D &= \frac{h}{2}\{[1 - \frac{\Psi(R_{750})}{R_{750}}](b-a)(u_5 - u_7) + (b-a)(u_5 - u_7)\} \\ &= \frac{h}{2}[2 - \frac{\Psi(R_{750})}{R_{750}}](b-a)(u_5 - u_7) \end{aligned} \tag{5.17}$$

It is obvious that both these contributions will be positive if the following inequality holds

$$0 \le \frac{\Psi(R)}{R} \le 2, \quad 0 \le \Psi(R) \le 2. \tag{5.18}$$

This means that a compressive limiter can be used in this case. However, this case is particularly simple: the grid is nicely structured and the advection velocity is constant. The case of unstructured grids and/or variable advection velocity is more complicated. ( The nonlinear case can be reduced for this purpose to the variable velocity case by using the multidimensional conservative linearization (see [2])).

Consider this general situation as illustrated in Fig.11. Assume that triangle $C$ is of Type II, while the neighboring (through the inflow faces of $C$) triangles $B$ and $C$ are of Type I. Collect, as before, the contributions to the updates at nodes 0 and 7 containing factors $(u_5 - u_0)$ and $(u_5 - u_7)$.

$$\begin{aligned} \phi_0^B + \phi_0^C &= \frac{h}{2}\{[1 - \Psi(R_{750})]k_0^C(u_5 - u_0) + k_0^B(u_5 - u_0)\} \\ &= \frac{h}{2}[(k_0^C + k_0^B) - \Psi(R_{750})k_0^C](u_5 - u_0) \end{aligned} \tag{5.19}$$

$$\begin{aligned} \phi_7^C + \phi_7^D &= \frac{h}{2}\{[1 - \frac{\Psi(R_{750})}{R_{750}}]k_7^C(u_5 - u_7) + k_7^D(u_5 - u_7)\} \\ &= \frac{h}{2}[(k_7^C + k_7^D) - \frac{\Psi(R_{750})}{R_{750}}k_7^C](u_5 - u_7) \end{aligned} \tag{5.20}$$

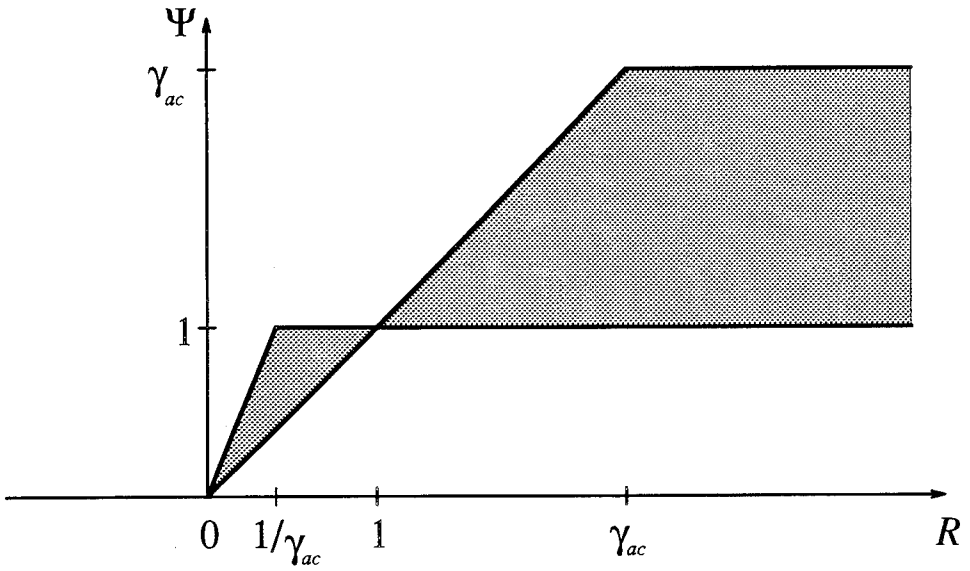


FIGURE 12. Positivity region for the limiter used in the NNL scheme.

where $k$'s are defined according to (4.7) (superscripts indicate the triangle). Defining the following 'artificial compression factor'

$$\gamma_{ac} = \min\left(\frac{k_7^C + k_7^D}{k_7^C}, \frac{k_0^C + k_0^B}{k_0^C}\right) \tag{5.21}$$

we can state

**Theorem 5.5.** *The NNL scheme is of the positive type if the limiter $\Psi(R)$ employed in triangle $C$ satisfies the following inequality*

$$0 \le \frac{\Psi(R)}{R} \le \gamma_{ac}, \quad 0 \le \Psi(R) \le \gamma_{ac}. \tag{5.22}$$

*Proof.* The proof is obvious from the previous argument. □

The *positivity region* (5.22) for the limiter function used with the $NNL$ scheme is illustrated on Fig.12. A class of limiters defined by

$$\Psi_\phi = \max(0, \min(\phi R, 1), \min(R, \phi)) \tag{5.23}$$

with the parameter $\phi$ satisfying

$$1 \le \phi \le \gamma_{ac}. \tag{5.24}$$

appears to suit this case very well. It is obvious that the choice

$$\phi = 1 \tag{5.25}$$

gives the minmod limiter which corresponds to the lower bound of the positivity region (Fig.12). The choice

$$\phi = \gamma_{ac}, \tag{5.26}$$

results in the "generalized" highly compressive Roe superbee limiter and corresponds to the upper bound of the positivity region (see Fig.12).

The amount of artificial compression that the scheme is allowed to use should probably be problem dependent. Usually it does not make much difference for the resolution of strong shocks and may lead to some undesirable effects in the smooth regions (for example, an advected sinusoidal wave may start looking like a square wave). However, it can make a great difference in resolving contact discontinuities.

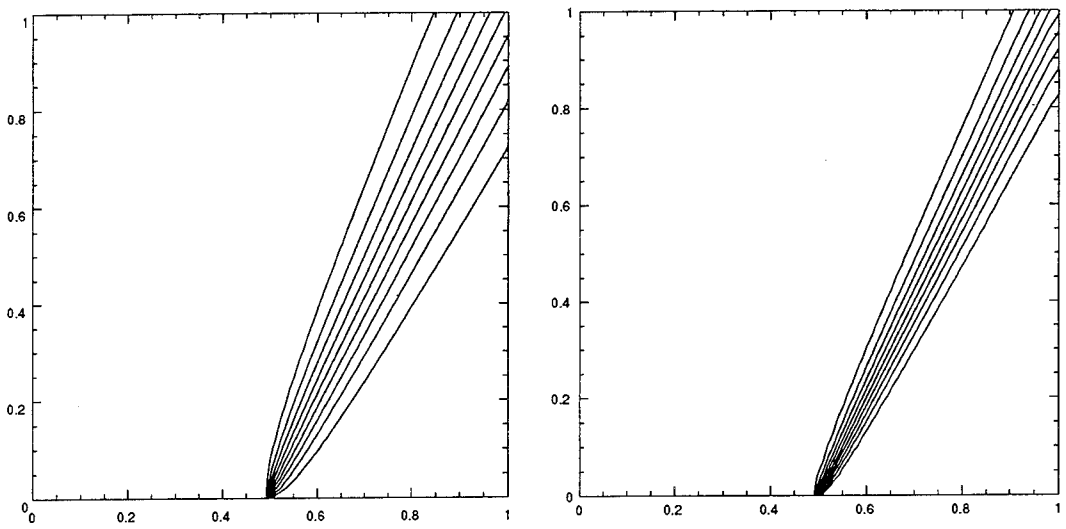


FIGURE 13. Regular upwinding and N scheme.

## 6. SOME NUMERICAL EXPERIMENTS

In this section we present some numerical experiments which illustrate the performance of the genuinely two-dimensional advection schemes. Two important aspects are considered: resolution of discontinuities and the accuracy in smooth regions. All testcases presented in this section consider the linear advection equation

$$u_t + u_y + .5u_x = 0.$$

6.1. **Resolution of discontinuities.** An extensive set of numerical experiments with the $S$ scheme concerning the resolution of discontinuities is presented in [15]. Here we shall illustrate this ability of the $S^*$ (or $NNL$) in comparison to the $S$ scheme.

We consider here the advection equation (6) on the square $[0,1]\times[0,1]$. The boundary conditions and the exact solution steady-state solution are given by

$$u = H(y - (2x - 2)),$$

where $H$ is the Heaviside function. The grid used is $50 \times 50$ points.

Figures13-16 present contour plots of the numerical solution to this problem obtained using different schemes. The performance of the first order regular upwind and the N schemes is illustrated by Fig.13. It can be observed that the N scheme is superior to the dimensional upwinding in terms of discontinuity resolution. However, the width of the numerical layer representing the discontinuity is $\mathcal{O}(h^{1/2})$ in both cases.

Fig.14 presents the results obtained by the $S$ and the $S^*$ (which is the same as $NNL$ scheme in this case) employing the non-compressive *minmod* limiter. Fig.15 corresponds to the same schemes except that the van Leer (harmonic mean) limiter is used. Experiments with the highly compressive *superbee* limiter are presented in Fig.16. It can be seen that the discontinuities are represented by sharp layers with no oscillations in the numerical obtained by both the $S$ and the $S^*$ schemes with all the three different limiters. Another conclusion is that the artificial compression may have a strong effect on the sharpness of such a layer. It can also be observed that the $S^*$ is slightly superior to the $S$ scheme in resolving contact discontinuities. This can be explained by its slightly narrower stencil.

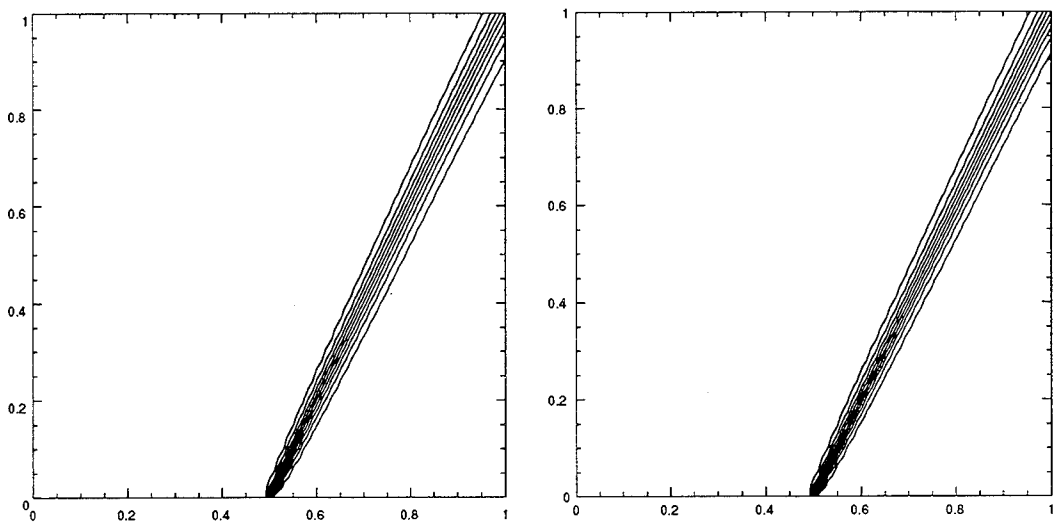


FIGURE 14. S and NNL scheme with "minmod" limiter.

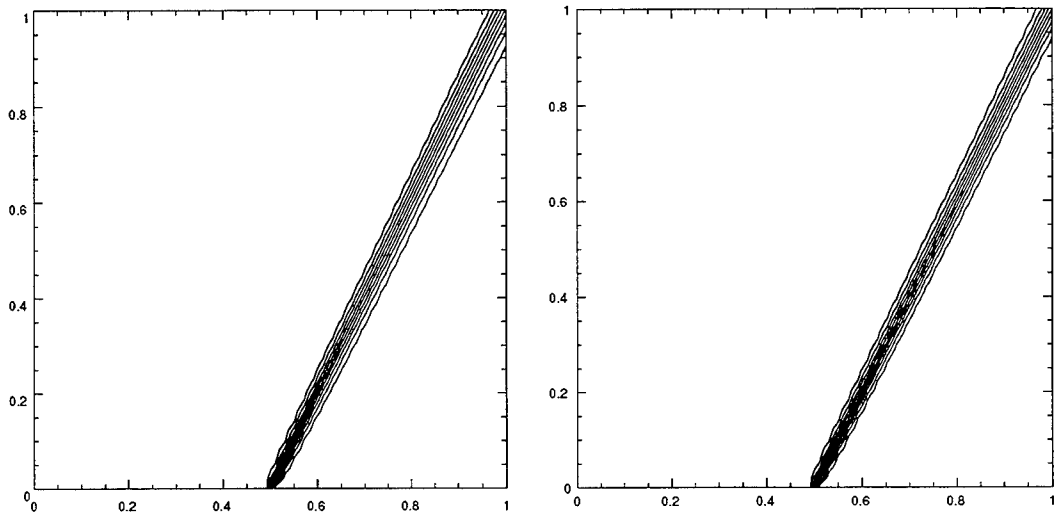


FIGURE 15. S and NNL scheme with van Leer limiter.

6.2. **Accuracy in smooth regions.** The purpose of the experiments presented here is to verify the accuracy of the $S^*$ (or the $NNL$ scheme on structured grid) in the smooth regions and to compare it to that of the $S$ scheme. An extensive set of numerical experiments with the $S$ employing different limiters was presented in [15]. Here we restrict our attention to the *minmod* limiter since the $S^*$ scheme (as well as the $NNL$ scheme in general unstructured grid case) satisfies the *local* positivity property in this case. Therefore, the treatment of each triangle is purely *local*. This results in a significantly more economical numerical algorithm, though at the expense of slightly inferior resolution of contact discontinuities.

The testcase considered is again the advection equation (6) on the square $[0,1] \times [0,1]$. The boundary conditions (and the exact steady-state solution) are given by

$$u = \sin(4x - 2y)$$

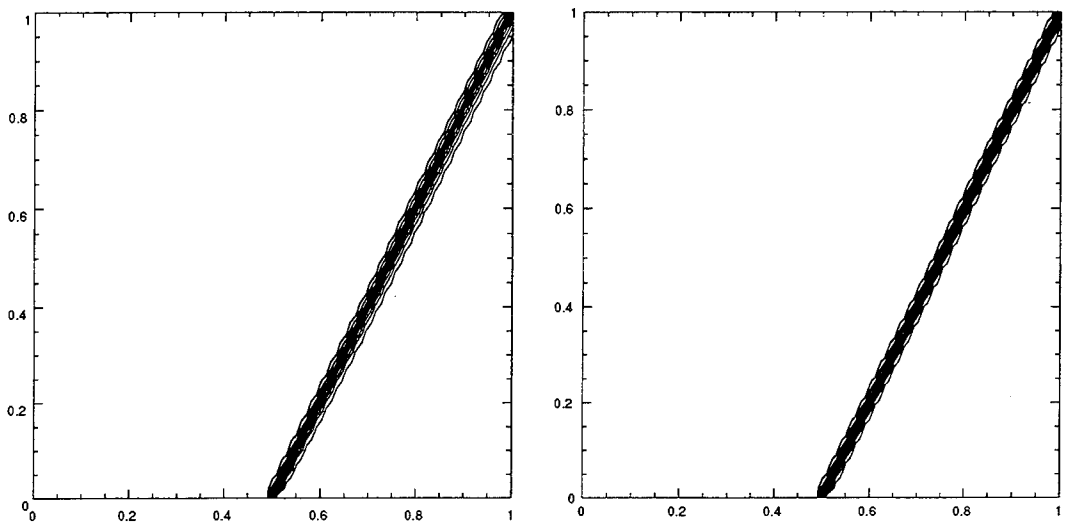


FIGURE 16. S and NNL scheme with Roe superbee limiter.

| gridsize | S scheme | S* scheme |
|---|---|---|
| 12×12 | $1.40 \times 10^{-2}$ | $1.17 \times 10^{-2}$ |
| 25×25 | $3.38 \times 10^{-3}$ | $2.69 \times 10^{-3}$ |
| 50×50 | $8.54 \times 10^{-4}$ | $6.73 \times 10^{-4}$ |

TABLE 1. $L_1$ solution error norm (measured on the $[0, 0.75] \times [0, 0.75]$ subdomain to avoid the influence of numerical boundary layers) for the problem $u_t + u_y + .5u_x = 0$ with the boundary conditions (and the exact steady-state solution) $u = \sin(4x - 2y)$.

The $L_1$ solution error norm measured on the subdomain $[0, 0.75] \times [0, 0.75]$ (to avoid any influence of the numerical boundary layers) is presented on Table 1 for the cases of the $S$ and $S^*$ schemes and three different levels of resolution.

The experiments with both schemes demonstrate second order accuracy at the steady-state of the both schemes. The solution error in the case of the $S^*$ scheme is slightly smaller than for the $S$ scheme. The explanation for this is the slightly narrower stencil of the $S^*$ scheme.

## 7. DISCUSSION AND CONCLUSIONS

This work establishes a link between two types of genuinely two-dimensional advection schemes. The truly two-dimensional schemes of the control volume type were constructed in [14],[15]. The fluctuation-splitting type schemes were introduced in [11],[3],[12],[17]. The $S^*$ scheme presented in this work can be interpreted as a representative of both classes. This allowed us to transfer ideas and insights between the two approaches and to combine the desirable properties of both classes in a single scheme. This is accomplished by the $NNL$ scheme, which on one hand (as a fluctuation-splitting scheme) is formulated on unstructured triangular grids. Thus, it allows for a simple treatment of complex geometries. On the other hand the $NNL$ scheme inherits the following properties of the control volume type genuinely multidimensional advection schemes:

- to use regular limiter functions in order to formulate the fluctuation-splitting schemes for unstructured triangular meshes;
- possibility to use artificial compression, which can improve the resolution of discontinuities;

- to formulate a fluctuation-splitting scheme having the LP property for the advection equation with nonzero forcing term.

One of the important objectives of this research direction is to construct highly efficient and robust multigrid steady-state solver for the compressible flow problems. The main motivation for constructing the multidimensional schemes of the control volume type in [14],[15] was to obtain a high-resolution scheme such that Gauss-Seidel relaxation (the simplest and very efficient smoother) is stable when applied directly to to the resulting discrete equations (which is not the case for dimensionally-split high-resolution schemes [16]). This made it possible to construct a highly efficient multigrid steady-state solver. The genuinely two-dimensional advection schemes formulated in this work ($S^*$ and $NNL$) inherit this property from their control volume type predecessors.

## References


1. H. Deconinck, Private communication.
2. H. Deconinck, P. L. Roe, and R. Struijs, *A multidimensional generalization of Roe's flux difference splitter for the Euler equations*, Comput. & Fluids **22** (1993), 215–222.
3. H. Deconinck, R. Struijs, and P. L. Roe, *Fluctuation splitting for multidimensional convection problem: an alternative to finite volume and finite element methods*, VKI Lecture Series 1990-3 on Computational Fluid Dynamics, Von Karman Institute, Brussels, Belgium, March 1991.
4. J. B. Goodman and R. J. LeVeque, *On the accuracy of stable schemes for two dimensional conservation laws*, Math. Comp. **45** (1985), 15–21.
5. Ch. Hirsch, *A general analysis of two-dimensional convection schemes*, VKI Lecture Series 1991-2 on Computational Fluid Dynamics, Von Karman Institute, Brussels, Belgium, February 1991.
6. Ch. Hirsch and P. van Ransbeeck, *Cell-centered multidimensional upwind algorithm and structured meshes*, Proc. ECCOMAS 1st European Computational Fluid Dynamics Conference, vol. 1, Elsevier, 1992, pp. 53–60.
7. B. Koren, *Low-diffusion rotated upwind schemes, multigrid and defect correction for steady, multi-dimensional euler flows*, Report NM-R 9021, CWI, Amsterdam, 1990.
8. B. Perthame, *Convergence of N-schemes for linear advection equations*, Proceedings of the Conference STAMM (Lisbon) (J. Rodriguez, ed.), 1994.
9. G. D. Raithby, *Skew upstream differencing schemes for problems involving fliud flow*, Comput. Methods Appl. Mech. Engrg. **9** (1976), 153–164.
10. J. Rice and R. Schnipke, *A monotone streamline upwind method for convection-dominated problems*, Comput. Methods Appl. Mech. Engrg. **48** (1985), 313–327.
11. P. L. Roe, *Linear advection schemes on triangular meshes*, CoA Report No. 8720, Cranfield Institute of Technology, Cranfield, Bedford, U.K., November 1987.
12. ———, *"Optimum" upwind advection on a triangular mesh*, Report No. 90-75, ICASE, 1990.
13. P. L. Roe and D. Sidilkover, *Optimum positive linear schemes for advection in two and three dimensions*, SIAM J. Numer. Anal. **29** (1992), 1542–1568.
14. D. Sidilkover, *Numerical solution to steady-state problems with discontinuities*, Ph.D. thesis, The Weizmann institute of Science, Rehovot, Israel, 1989.
15. D. Sidilkover and A. Brandt, *Multigrid solution to steady-state 2d conservation laws*, SIAM J. Numer. Anal. **30** (1993), 249–274.
16. S. Spekreijse, *Multigrid solution of monotone second-order discretization of hyperbolic conservation laws*, Math. Comp. **49** (1987), 135–155.
17. R. Struijs, H. Deconinck, P. de Palma, P. L. Roe, and K. G. Powell, *Progress on multidimensional upwind Euler solvers for unstructured grids*, AIAA 91-1550, June 24-26 1991, Honolulu, Hawai.
18. P. Sweby, *High resolution schemes using flux limiters for hyperbolic conseravtion laws*, SIAM J. Numer. Anal. **21** (1984), 995–1011.

## Appendix.

### Appendix A. S scheme - general inhomogeneous case

Consider the following scheme

$$\begin{aligned} f^{2D}{}_- &= au_3 - \tfrac{1}{2}(b(u_3-u_4) - hs^f_-) \\ g^{2D}{}_- &= bu_5 - \tfrac{1}{2}(a(u_5-u_4) - hs^g_-). \end{aligned} \tag{A.1}$$

It has been shown in [14],[15] that the 2D scheme is second order accurate at steady state for inhomogeneous equation. The definition of $s^f_-, s^g_-$ is non-unique (see [14],[15]). We consider here one particular choice which appears to be of particular importance for the purpose of this work (see Appendix B):

$$s^f_- = \frac{2}{3}s_3 + \frac{1}{3}s_4 \tag{A.2}$$

$$s^g_- = \frac{2}{3}s_5 + \frac{1}{3}s_4 \tag{A.3}$$

If one is content to obtain first order accuracy the previously defined N scheme can be used. However, the purpose of it here is to serve as an intermediate step towards the construction of the second order accurate S* scheme. Therefore, we shall modify it. For our representative case $a < b$, putting

$$\beta = \min(1, \frac{a}{b}) = \frac{a}{b} < 1, \tag{A.4}$$

and defining

$$s_- = \frac{1}{3}(s_0 + s_3 + s_4) \tag{A.5}$$

the N scheme can be given by:

$$\begin{aligned} f^N{}_- &= au_3 - \tfrac{1}{2}\{a(u_3-u_4) - h[s^f_- - (1-\beta)s_-]\} \\ g^N{}_- &= bu_5 - \tfrac{1}{2}(a(u_5-u_4) - hs^g_-). \end{aligned} \tag{A.6}$$

The S* scheme is defined by

$$\begin{aligned} f^S{}_- &= f^S{}_- - \tfrac{1}{2}\Psi(R_{043})((b-a)(u_3-u_4) - (1-\beta)hs^-) \\ g^S{}_- &= g^S{}_- \end{aligned} \tag{A.7}$$

where

$$R_{043} = -\frac{a(u_0-u_4) - \beta hs_-}{(b-a)(u_3-u_4) - (1-\beta)hs_-} \tag{A.8}$$

The update formula in this case

$$\begin{aligned} u_0^{n+1} = u_0^n + \frac{\Delta t}{h}\{ & b(u_5-u_0) + a(u_4-u_5) \\ & -\frac{1}{2}\Psi(R_{750})[(b-a)(u_5-u_0) + h(1-\beta)s_-] \\ & +\frac{1}{2}\Psi(R_{043})[(b-a)(u_4-u_3) + h(1-\beta)s_+] \\ & +\frac{h}{2}[s^f_+ - s^f_- + s^g_+ - s^g_+ + (1-\beta)(s_+ - s_-)]\} \end{aligned} \tag{A.9}$$

or

$$u_0^{n+1} = u_0^n + \frac{\Delta t}{h}\{ \quad b(u_5 - u_0) + a(u_4 - u_5)$$
$$-\frac{1}{2}\Psi(R_{750})[(b-a)(u_5 - u_0) + h(1-\beta)s_-]$$
$$+\frac{1}{2}\Psi(R_{043})[(b-a)(u_4 - u_3) + h(1-\beta)s_+]$$
$$+\frac{h}{2\cdot 3}[2s_0 + (1-\beta)s_3 + (2-\beta)s_4 + (1+\beta)s_5 + \beta s_7]\} \tag{A.10}$$

**Lemma A.1.** *If $\Psi = \Psi(R)$ is Lipschitz continuous and*

$$\Psi(1) = 1, \tag{A.11}$$

*then the S* scheme is second order accurate.*

*Proof.* Note that

$$\begin{aligned}
& (f_+^S - f_-^S) - (f_+^{2D} - f_-^{2D}) \\
= \; & (1 - \Psi(R_{750}))((b-a)(u_0 - u_5) - \beta h s_+) \\
& -(1 - \Psi(R_{043}))((b-a)(u_3 - u_4) - \beta h s_-) \\
= \; & h(\Psi(R_{043}) - \Psi(R_{750}))((b-a)(u_y - .5hu_{yy}) - \beta s) \\
& +h^2(1 - \Psi(R_{043}))((b-a)u_{xy} - \beta s_x) \\
& +\mathcal{O}(h^3)
\end{aligned} \tag{A.12}$$

The second order accuracy of the S* scheme requires:

$$1 - \Psi(R_{043}) = \mathcal{O}(h) \tag{A.13}$$

and

$$\Psi(R_{043}) - \Psi(R_{750}) = \mathcal{O}(h^2) \tag{A.14}$$

$$\begin{aligned}
R_{043} &= -\frac{a(u_0 - u_4) - \beta h s_-}{(b-a)(u_3 - u_4) - (1-\beta)hs_-} \\
&= 1 - \frac{a(u_0 - u_4) + (b-a)(u_3 - u_4) - hs_-}{(b-a)(u_3 - u_4) - (1-\beta)hs_-} \\
&= 1 - \frac{(au_x + bu_y - s) - .5hbu_{yy} - .5hau_{xx} - hbu_{xy} - .5hs_x}{(b-a)u_y - (1-\beta)s + \mathcal{O}(h)} + \mathcal{O}(h^2) \\
&= 1 - h\frac{-.5bu_{yy} - .5au_{xx} - bu_{xy} - .5s_x}{(b-a)u_y - (1-\beta)s} + \mathcal{O}(h^2)
\end{aligned} \tag{A.15}$$

Similarly

$$R_{750} = 1 - h\frac{-.5bu_{yy} + .5au_{xx} + .5s_x}{(b-a)u_y - (1-\beta)s} + \mathcal{O}(h^2) \tag{A.16}$$

Therefore

$$1 - R_{043} = \mathcal{O}(h) \tag{A.17}$$

and

$$R_{750} - R_{043} = h\frac{(au_x + bu_y - s)_x}{(b-a)u_y - (1-\beta)s} + \mathcal{O}(h^2) = \mathcal{O}(h^2). \tag{A.18}$$

Then because $\Psi$ is Lipschitz continuous

$$1 - \Psi(R_{043}) = (1 - \Psi(1)) + \mathcal{O}(h) \tag{A.19}$$

and

$$\Psi(R_{750}) - \Psi(R_{043}) = \mathcal{O}(h^2), \tag{A.20}$$

which together with the fact that the 2D scheme is second order accurate proves the lemma. □

## Appendix B. Fluctuation-splitting scheme for the inhomogeneous case

Here we address the problem of maintaining linearity preserving property the NNL scheme on unstructured triangular meshes in the case of non-zero forcing term. Consider again the inhomogeneous advection equation (4.1). The N scheme given by (4.16),(4.17) for the homogeneous case should be now modified. One target formula (Type I triangle, Fig.7) now is

$$S_3 u_3^{n+1} = S_3 u_3^n + \Delta t[k_1(u_1 - u_3) + k_2(u_2 - u_3) - \sigma_T] \tag{B.1}$$

and in two target case (Type II triangle, Fig.7)

$$\begin{aligned} S_1 u_1^{n+1} &= S_1 u_1^n + \Delta t[k_1(u_1 - u_3) - \beta\sigma_T] \\ S_2 u_2^{n+1} &= S_2 u_2^n + \Delta t[k_2(u_2 - u_3) - (1-\beta)\sigma_T], \end{aligned} \tag{B.2}$$

where

$$\beta = \frac{k_1}{k_1 + k_2} \tag{B.3}$$

and $\sigma_T$ defined by (4.4). The following distribution formulae will give the inhomogeneous NNL scheme in the two target case

$$\begin{aligned} S_1 u_1^{n+1} = S_1 u_1^n + \Delta t\{[ \;& k_1(u_1 - u_3) - \beta\sigma_T] \\ & + \Psi(R_{132})[k_2(u_2 - u_3) - (1-\beta)\sigma_T]\} \\ S_2 u_2^{n+1} = S_2 u_2^n + \Delta t\{[ \;& k_2(u_2 - u_3) - (1-\beta)\sigma_T] \\ & - \Psi(R_{132})[k_2(u_2 - u_3) - (1-\beta)\sigma_T]\}, \end{aligned} \tag{B.4}$$

where

$$R_{132} = -\frac{k_1(u_1 - u_3) - \beta\sigma_T}{k_2(u_2 - u_3) - (1-\beta)\sigma_T} \tag{B.5}$$

Identity

$$\Psi(R_{132})[k_2(u_2 - u_3) - (1-\beta)\sigma_T] \equiv -\frac{\Psi(R_{132})}{R_{132}}[k_1(u_1 - u_3) - \beta\sigma_T] \tag{B.6}$$

Positivity of this scheme can be demonstrated in the same way as for the homogeneous equation. The following result concerning the LP property of the constructed scheme can be formulated

**Theorem B.1.** *The NNL scheme (B.1),(B.2) is linearity preserving in the inhomogeneous case if*

$$|\Psi(R) - 1| < C|R - 1| \tag{B.7}$$

*for some positive constant $C$.*

*Proof.* Define

$$\begin{aligned} \delta u_1 &= S_1 u_1^{n+1} - S_1 u_1^n \\ &= \Delta t\{[k_1(u_1 - u_3) - \beta\sigma_T] + \Psi(R_{132})[k_2(u_2 - u_3) - (1-\beta)\sigma_T]\} \\ &= P + \Psi(R)Q \end{aligned} \tag{B.8}$$

$$\begin{aligned} \delta u_2 &= S_2 u_2^{n+1} - S_2 u_2^n \\ &= \Delta t\{[k_2(u_2 - u_3) - (1-\beta)\sigma_T] - \Psi(R_{132})[k_2(u_2 - u_3) - (1-\beta)\sigma_T]\} \\ &= Q - \Psi(R)Q. \end{aligned}$$

The rest of the proof is the same as of Theorem 5.3. □

To demonstrate the connection between the inhomogeneous NNL scheme and previously constructed S* scheme consider the grid illustrated in Fig.9. The fluctuations from the triangles $A, B, C$ can be given by the following formulae

$$
\begin{aligned}
\phi^A &= -\tfrac{h}{2}\{\ [1-\Psi(R_{043})][(b-a)(u_3-u_4)-(1-\beta)hs^A] \\
&\quad +\underline{a(u_0-u_4)-\beta hs^A}+\underline{\Psi(R_{043})[(b-a)(u_3-u_4)-(1-\beta)hs^A]}\} \\
\phi^B &= -\tfrac{h}{2}\{\ \underline{a(u_0-u_4)}+\underline{(b-a)(u_0-u_5)-hs^B}\} \\
\phi^C &= -\tfrac{h}{2}\{\ \underline{a(u_7-u_5)}-\beta hs^C+\Psi(R_{750})[(b-a)(u_0-u_5)-(1-\beta)hs^C] \\
&\quad +\underline{[1-\Psi(R_{750})][(b-a)(u_0-u_5)-(1-\beta)hs^C]}\},
\end{aligned}
\tag{B.9}
$$

where the underlined terms contribute to the residual at the node 0. Thus the update formula is

$$
\begin{aligned}
u_0^{n+1} = u_0^n + \frac{\Delta t}{h}\{\quad & b(u_5-u_0)+a(u_4-u_5) \\
& -\frac{1}{2}\Psi(R_{750})[(b-a)(u_5-u_0)+h(1-\beta)s_C] \\
& +\frac{1}{2}\Psi(R_{043})[(b-a)(u_4-u_3)+h(1-\beta)s_A] \\
& +\frac{h}{2}[s_B+(1+\beta)s_A+(1-\beta)s_C]\}.
\end{aligned}
\tag{B.10}
$$

Recalling the definition of $s_A, s_B, s_C$ it is easy to see that (B.10) is identical to (A.10).

ICASE, Mail Stop 132C, NASA Langley Research Center, Hampton, VA 23681
*E-mail address*: sidilkov@@icase.edu

Department of Aerospace Engineering, University of Michigan, Ann Arbor, MI 48109.
*E-mail address*: philroe@@engin.umich.edu

# REPORT DOCUMENTATION PAGE

*Form Approved*
*OMB No. 0704-0188*



| 1. AGENCY USE ONLY *(Leave blank)* | 2. REPORT DATE | 3. REPORT TYPE AND DATES COVERED |
|---|---|---|
| | February 1995 | Contractor Report |

**4. TITLE AND SUBTITLE**
UNIFICATION OF SOME ADVECTION SCHEMES IN TWO DIMENSIONS

**5. FUNDING NUMBERS**
C NAS1-19480
WU 505-90-52-01

**6. AUTHOR(S)**
D. Sidilkover
P. L. Roe

**7. PERFORMING ORGANIZATION NAME(S) AND ADDRESS(ES)**
Institute for Computer Applications in Science
and Engineering
Mail Stop 132C, NASA Langley Research Center
Hampton, VA 23681-0001

**8. PERFORMING ORGANIZATION REPORT NUMBER**
ICASE Report No. 95-10

**9. SPONSORING/MONITORING AGENCY NAME(S) AND ADDRESS(ES)**
National Aeronautics and Space Administration
Langley Research Center
Hampton, VA 23681-0001

**10. SPONSORING/MONITORING AGENCY REPORT NUMBER**
NASA CR-195044
ICASE Report No. 95-10

**11. SUPPLEMENTARY NOTES**
Langley Technical Monitor: Dennis M. Bushnell
Final Report
Submitted to Math. Comp.

**12a. DISTRIBUTION/AVAILABILITY STATEMENT**
Unclassified–Unlimited

Subject Category 64

**12b. DISTRIBUTION CODE**

**13. ABSTRACT** *(Maximum 200 words)*
In this paper a relationship between two approaches towards construction of genuinely two-dimensional upwind advection schemes is established. One of these approaches is of the control volume type applicable on structured cartesian meshes. It resulted (see [14], [15]) in the compact high resolution schemes capable of maintaining second order accuracy in both homogeneous and inhomogeneous cases. Another one is the fluctuation splitting approach (see [11], [3], [12], [17]), which is well suited for triangular (and possibly) unstructured meshes. Understanding the relationship between these two approaches allows us to formulate here a new fluctuation splitting high resolution (i.e. possible use of artificial compression, while maintaining positivity property) scheme. This scheme is shown to be linearity preserving in inhomogeneous as well as homogeneous cases.

| 14. SUBJECT TERMS | 15. NUMBER OF PAGES |
|---|---|
| multidimensional advection; non-zero forcing term; structural and unstructural meshes | 28 |
| | 16. PRICE CODE A03 |

| 17. SECURITY CLASSIFICATION OF REPORT | 18. SECURITY CLASSIFICATION OF THIS PAGE | 19. SECURITY CLASSIFICATION OF ABSTRACT | 20. LIMITATION OF ABSTRACT |
|---|---|---|---|
| Unclassified | Unclassified | | |